

Hippocampal-specific insulin resistance elicits behavioral despair and hippocampal dendritic atrophy



L.P. Reagan^{a,b}, H.B. Cowan^b, J.L. Woodruff^{a,b}, G.G. Piroli^b, J.M. Erichsen^b, A.N. Evans^b, H. E. Burzynski^b, N.D. Maxwell^b, F.Z. Loyo-Rosado^b, V.A. Macht^{b,1}, C.A. Grillo^{a,b,*}

^a Columbia VA Health Care System, Columbia, SC, 29209, USA

^b University of South Carolina School of Medicine, Department of Pharmacology, Physiology, and Neuroscience, Columbia, SC, 29209, USA

ARTICLE INFO

Keywords:
Diabetes
Obesity
Depression
Anxiety
Hippocampal plasticity
Insulin receptor

ABSTRACT

Insulin resistance is a major contributor to the neuroplasticity deficits observed in patients with metabolic disorders. However, the relative contribution of peripheral versus central insulin resistance in the development of neuroplasticity deficits remains equivocal. To distinguish between peripheral and central insulin resistance, we developed a lentiviral vector containing an antisense sequence selective for the insulin receptor (LV-IRAS). We previously demonstrated that intra-hippocampal injection of this vector impairs synaptic transmission and hippocampal-dependent learning and memory in the absence of peripheral insulin resistance. In view of the increased risk for the development of neuropsychiatric disorders in patients with insulin resistance, the current study examined depressive and anxiety-like behaviors, as well as hippocampal structural plasticity in rats with hippocampal-specific insulin resistance. Following hippocampal administration of either the LV-control virus or the LV-IRAS, anhedonia was evaluated by the sucrose preference test, despair behavior was assessed in the forced swim test, and anxiety-like behaviors were determined in the elevated plus maze. Hippocampal neuron morphology was studied by Golgi-Cox staining. Rats with hippocampal insulin resistance exhibited anxiety-like behaviors and behavioral despair without differences in anhedonia, suggesting that some but not all components of depressive-like behaviors were affected. Morphologically, hippocampal-specific insulin resistance elicited atrophy of the basal dendrites of CA3 pyramidal neurons and dentate gyrus granule neurons, and also reduced the expression of immature dentate gyrus granule neurons. In conclusion, hippocampal-specific insulin resistance elicits structural deficits that are accompanied by behavioral despair and anxiety-like behaviors, identifying hippocampal insulin resistance as a key factor in depressive illness.

1. Introduction

Insulin plays a critical role in maintaining peripheral glucose homeostasis through activation of insulin receptors expressed in peripheral tissues. While glucose homeostasis in the central nervous system (CNS) is proposed to be less dependent upon insulin receptor activation, neuronal insulin receptor signaling plays a critical role in the development and maintenance of neuroplasticity beginning at the earliest stages of development (Ferrario and Reagan, 2018). In this regard, insulin promotes synapse formation (Chiu and Cline, 2010), regulates the expression and trafficking of glutamate receptor subunits (Skeberdis et al., 2001) and facilitates synaptic transmission (Chen and Leonard,

2002). Moreover, intracerebroventricular (Park et al., 2000), as well as intrahippocampal administration (McNay et al., 2010; Moosavi et al., 2006) of insulin increases performance on learning and memory tasks in rodents. Collectively, these studies support the hypothesis that beyond the well-described metabolic effects in the periphery, insulin in the CNS promotes synaptic plasticity.

The neuroplasticity activities of insulin are in stark contrast to the impairments in neuroplasticity observed in brain insulin resistance associated with metabolic disorders like diabetes and obesity, as well as dementia and Alzheimer's disease (AD) (Biessels and Reagan, 2015). Indeed, brain insulin resistance has been identified as a core feature of AD (Talbot et al., 2012; Bomfim et al., 2012). Beyond cognitive deficits,

* Corresponding author. Department of Pharmacology, Physiology and Neuroscience University of South Carolina School of Medicine, 6439 Garners Ferry Road, D47, Columbia, SC, 29209, USA

E-mail address: cgrillo@uscmed.sc.edu (C.A. Grillo).

¹ Present address: Bowles Center for Alcohol Studies, The University of North Carolina at Chapel Hill, Chapel Hill, NC, USA, 27599.

<https://doi.org/10.1016/j.ynstr.2021.100354>

Received 8 March 2021; Received in revised form 4 June 2021; Accepted 11 June 2021

Available online 16 June 2021

2352-2895/© 2021 The Authors

Published by Elsevier Inc.

This is an open access article under the CC BY-NC-ND license

(<http://creativecommons.org/licenses/by-nd/4.0/>).

epidemiological studies identified brain insulin resistance as a risk factor for the development of neuropsychiatric disorders like depressive illness (Anderson et al., 2001; Ali et al., 2006; Lustman and Clouse, 2005). Similarly, depressive-like behaviors are observed in experimental models of type 2 diabetes mellitus (T2DM) and obesity (Collin et al., 2000; Yamada et al., 2011; Sharma et al., 2010; Grillo et al., 2011a), which are characterized by insulin resistance. Collectively, these results support the hypothesis that brain insulin resistance impairs synaptic plasticity, cognition and mood. However, these studies cannot assess whether brain insulin resistance is a cause or a consequence of the neuroplasticity deficits associated with metabolic disorders and age-related cognitive decline. Moreover, these studies cannot distinguish between the effects of peripheral versus brain insulin resistance in the development of neuroplasticity deficits observed in metabolic disorders (Grillo et al., 2019). To address this issue, we have developed and characterized a lentiviral vector containing an antisense sequence selective for the insulin receptor. We have previously shown that hippocampal administration of this viral vector elicits impairments in hippocampal-dependent learning and memory and hippocampal neuroplasticity in the absence of changes in peripheral glucose homeostasis or insulin sensitivity (Grillo et al., 2015a). As the hippocampus has been defined as a CNS epicenter in the pathophysiology of neuropsychiatric disorders, the aim of the current studies was to examine morphological plasticity and the development of depressive-like and anxiety-like behaviors in rats with hippocampal-specific insulin resistance. These results provide new insights into the underlying morphological changes that contribute to neurobehavioral deficits in brain insulin resistance states.

2. Methods and materials

2.1. Animal protocols

Adult male Sprague Dawley rats (CD strain, Envigo) weighing 200–250 g were individually housed and provided *ad libitum* access to food and water. All procedures were performed in accordance with all guidelines and regulations of the Dorn VA Animal Care and Use Committee. Stereotaxic surgery to inject either the control lentivirus (LV-Con) or a lentivirus containing an antisense sequence selective for the insulin receptor (LV-IRAS) into the hippocampus was performed as described in our previous studies (Grillo et al., 2015a). Briefly, rats under isoflurane anesthesia were placed in the stereotaxic apparatus and lentivirus was injected into the dorsal hippocampus at the following coordinates: AP: 4.8 mm, L: ± 4.0 mm, and DV: 3.0 mm. Using a 10 μ l Hamilton syringe driven by a motorized stereotaxic injector (Stoelting 53310), 5 μ l of the viral stock (5×10^6 tu/ μ l) were injected at a speed of 0.2 μ l/min for 25 min; the needle was left in place for an additional 15 min. For a detailed map of this viral construct, please see [Supplemental Figure 1](#). Two distinct cohorts of rats were used in these studies. For behavioral analyses, twenty rats received bilateral intrahippocampal injections of either the LV-Con construct ($n = 10$) or the LV-IRAS construct ($n = 10$). For the Golgi-impregnation studies, a separate cohort of five rats received an intrahippocampal injection of the LV-Con construct in one hemisphere and an intrahippocampal injection of the LV-IRAS construct into the contralateral hemisphere; hemispheres that received the LV-IRAS construct were counter-balanced. This design allowed each rat to serve as its own control for the morphological analyses. Hemispheres that received the LV-Con construct are referred to as Hippo-Con; hemispheres that received the LV-IRAS construct are referred to as Hippo-IRAS. After surgery, rats were housed in a BSL2 facility for at least four weeks prior to subsequent analyses.

2.2. Immunoblot analysis

Immunoblotting analysis was performed as described in our previous studies (Grillo et al., 2015a). Briefly, membrane fractions, prepared from

the whole hippocampus, were separated by SDS/PAGE (10%), transferred to polyvinylidene difluoride (PVDF) membranes, and blocked in TBS plus 10% non-fat dry milk plus 0.05% Tween 20 for 60 min. PVDF membranes were incubated with insulin receptor primary antisera (Cell Signaling Technologies Cat #3021; 1:1000 dilution) in TBS/5% non-fat dry milk/0.05% Tween 20. After overnight incubation at 4 °C, blots were washed and incubated with peroxidase-labeled species-specific secondary antibodies. PVDF membranes were then washed with TBS/5% non-fat dry milk/0.05% Tween 20 and developed using enhanced chemiluminescence reagents (ECL, Amersham) as described by the manufacturer. Normalization for protein loading was performed using a mouse monoclonal primary antibody selective for actin (Sigma Chemical Cat #A5441; 1:50,000 dilution). Chemiluminescent signals were captured on photographic film (Electron Microscopy Sciences, Hatfield, PA). Images from the films were captured using an Epson Perfection V600 scanner at a resolution of 300 dpi and saved as TIFF files. The software Image J (NIH) was used for the quantification of band intensities by densitometry (Tanus et al., 2015).

2.3. Micro CT image acquisition

CT scans were collected using a Quantum GX microCT Imaging System (PerkinElmer) on prone rats anesthetized with isoflurane. Scans were collected over 2 min at 90 kV and 88 μ A using an aluminum 1.0 X-Ray filter. We targeted the L1 to L5 region of the spinal cord during the scan with an 86 mm field of view. Caliper Analyze version 12.0 was used to analyze the CT scans. The images were first cropped at L1 and L5 to ensure fair comparisons between samples. Applying a median filter 3 and then a low pass filter 3 smoothed the image to show a clear abdominal wall that could be delineated from the surrounding adipose tissue. The volume edit tool was then used to separate different tissue groups based on density thresholding. Thresholding values were set based on landmarks for different tissue groups: vertebral column or ribs for bone, kidneys for soft tissue, and subcutaneous fat pads for fat. Subcutaneous fat was manually separated from the visceral fat using the abdominal wall as a separation between the two fat pads. Total volume was then automatically measured for the two fat groups.

2.4. Plasma endocrine analysis

Enzyme-linked immunosorbent assay (ELISA) analysis was performed for corticosterone (Enzo Life Sciences, Farmingdale, NY), leptin and insulin (Millipore, Billerica, MA) in plasma isolated from Hippo-Con and Hippo-IRAS rats. ELISA plates were analyzed according to the manufacturer's instructions using a Synergy 2 Gen 5 microplate reader (BioTek Instruments, Winooski, Vermont). Plasma triglycerides were determined using an enzymatic kit (modified Trinder) according to the manufacturer's instructions (Pointe Scientific, Inc., Canton, MI, USA). Blood glucose was assessed using a glucometer.

2.5. Behavioral analyses

As described in our previous studies, anhedonia was evaluated using the sucrose preference test, behavioral despair was evaluated in the forced swim test (FST), and anxiety-like behavior was assessed in the elevated plus maze (EPM); see (Grillo et al., 2011a; Macht et al., 2017) for detailed descriptions of these assays. Data from the two-bottle (water versus 1% sucrose solution) anhedonia test were expressed as the ratio of sucrose intake/sucrose + water intake (i.e., sucrose preference). Fluid intake was measured 1 h after the start of the dark phase on both the pre-test (i.e., habituation) day and the test day. Endpoint measures in the EPM included time spent in open and closed arms, entries into open and closed arms, center time, and distance traveled. In the FST, endpoint measures on both the pre-test day and the test day included latency to immobility, duration of immobility, swimming and climbing.

2.6. Immunohistochemistry for doublecortin

Rat brains were prepared for immunohistochemical analysis as described in our previous studies (Grillo et al., 2015a). Briefly, rat brain sections were washed with 0.1 M PBS and then incubated with primary antisera raised against doublecortin (DCX, 1:500 dilution; Santa Cruz Biotechnology, Inc.). Following an overnight incubation at 4 °C, sections were washed in PBS and then incubated in biotinylated donkey anti-rabbit secondary antibody (1:600) for 90 min at room temperature (RT). Following washes with PBS, sections were incubated with horseradish peroxidase-conjugated streptavidin (Vector Laboratories; 1:100) at RT for 1 h. DCX immunoreactivity was developed using diaminobenzidine as substrate. A blinded operator counted all the DCX-positive neurons in the superior and inferior blades of the dentate gyrus of six rats per group using two representative sections, at least 280 μm apart, from similar rostral-caudal planes in the proximity of the virus infusion site (4.20–5.00 mm posterior from bregma).

2.7. Morphological analysis

Rat brains were processed for a modification of the Golgi-Cox technique using the FD Rapid Golgi Stain Kit protocol (FD Neuro Technologies, Ellicot City, MD) as described in our previous studies (Grillo et al., 2015b). The three-dimensional analysis of dendritic morphology was performed using a computer-based tracing system (Neurolucida/Neuroexplorer; MicroBrightField, Inc.). Neurons were selected using established criteria for this type of analysis, as described in (Grillo et al., 2015b). At least six neurons were randomly selected and analyzed from each hippocampal hemisphere in each rat. Five rats were used in this study. The neuron summary analysis was performed with Neurolucida Explorer (MBF Bioscience) and involved the following measurements: (a) total dendritic length, (b) number of dendritic branch points and (c) total dendritic volume. Additionally, the Dendritic Complexity Index (DCI) was calculated using the Neurolucida software as follows: DCI = (Σ branch tip orders + number branch tips) × (total dendritic length/total number of primary dendrites). Branch tip order is determined by the number of bifurcations in a particular dendritic segment between a particular terminal tip and the cell body (Pillai et al., 2012).

2.8. Fluoro-Jade histochemistry

Fluoro-Jade histochemistry was performed as described in our previous studies (Grillo et al., 2007). Briefly, coronal brain sections from Hippo-Con and Hippo-IRAS rats were cut at a thickness of 16 μm on a cryostat microtome and mounted on gelatin-coated slides; coronal brain sections from adrenalectomized (ADX) rats were used as positive controls for Fluoro-Jade labeling. Sections were briefly dried and then washed and incubated with 0.05% potassium permanganate for 15 min at RT. Slides were washed and incubated with 0.001% Fluoro-Jade C (Histochem International) in HPLC-grade water. Sections were then washed in HPLC-grade water, dried on a slide warmer, dehydrated with xylenes, and cover-slipped with Permount.

2.9. Statistical analysis

For all endpoint measures, statistical analysis was performed using an unpaired *t*-test with a *p* < 0.05 as the criterion for statistical significance.

3. Results

3.1. Validation of lentivirus efficacy

The efficacy of the LV-IRAS construct to downregulate hippocampal insulin receptor signaling was assessed by immunoblot analysis for the insulin receptor (IR) in hippocampal total membrane extracts. In

agreement with our previous studies (Grillo et al., 2015a), insulin receptor expression was significantly decreased in hippocampal extracts prepared from rats that received the LV-IRAS construct (Hippo-IRAS) compared to rats that received the LV-Con (Hippo-Con) construct (Fig. 1A); autoradiographic analysis confirmed this observation (Fig. 1B). These decreases in hippocampal insulin receptor expression were not accompanied by alterations in plasma endocrine measures (Supplementary Table 1), changes in body weight (Fig. 1C) or changes in visceral (Fig. 1E) or subcutaneous fat (Fig. 1F). Collectively, these results confirm our previous observations that intra-hippocampal administration of the LV-IRAS construct elicits downregulation of hippocampal insulin receptors in the absence of changes in body weight, body composition, peripheral insulin resistance or plasma endocrine measures.

3.2. Hippocampal-specific insulin resistance elicits behavioral despair and anxiety-like behaviors

To assess the effects of hippocampal-specific insulin resistance on behavioral despair and anhedonia, the FST and the sucrose preference test were performed in Hippo-Con and Hippo-IRAS rats. On the pre-test day of the FST, immobility, swimming and climbing behaviors did not differ between Hippo-Con and Hippo-IRAS rats (data not shown). However, on the test day of the FST, Hippo-IRAS rats exhibited significant increases in immobility (Fig. 2A) and decreased latency to float (Fig. 2B). Corresponding decreases in active behaviors in the FST were selective for climbing; specifically, climbing behaviors were significantly decreased in Hippo-IRAS rats compared to Hippo-Con rats (Fig. 2C), while swimming behaviors were not significantly different between the groups (Fig. 2D). In the anhedonia test, total fluid intake (Hippo-Con: 6.1 ± 0.5 ml; Hippo-IRAS: 6.9 ± 1.0 ml; *p* = 0.57) and sucrose preference (Hippo-Con: 95.73% ± 0.88; Hippo-IRAS: 93.56% ± 2.08; *p* = 0.33) did not differ in Hippo-IRAS rats compared to Hippo-Con rats. In the EPM, while time spent in the closed arms (Fig. 2E), time spent in the maze center (Fig. 2G), and total distance (Fig. 2H) did not differ between Hippo-Con and Hippo-IRAS rats, open arm time was significantly reduced in Hypo-IRAS rats (Fig. 2F). Overall, these results indicate that Hippo-IRAS rats exhibit behavioral despair in the FST and anxiety-like behaviors in the EPM in the absence of anhedonic responses.

3.3. Hippocampal insulin resistance decreases the density of immature granule neurons in the absence of neurodegeneration

The expression of doublecortin (DCX), a marker of immature granule neurons in the dentate gyrus (DG), was examined as a measure of morphological plasticity in Hippo-Con and Hippo-IRAS rats. Immunohistochemical analysis revealed the expected profile for DCX expression in the DG in rats that received the LV-Con construct (Fig. 3A and C) or the LV-IRAS construct (Fig. 3B and D). Non-biased stereological analysis determined that the number of cells expressing DCX was significantly reduced in the superior blade (DGs) and the inferior blade (DGi) of the DG in Hippo-IRAS rats compared to Hippo-Con rats (Fig. 3E). Conversely, Fluoro-Jade histochemical analysis did not identify degenerating neurons in the hippocampus of Hippo-Con or Hippo-IRAS rats (Supplemental Figure 2), indicating that hippocampal-specific insulin resistance was not accompanied by hippocampal neurodegeneration.

3.4. Hippocampal insulin resistance induces hippocampal dendritic atrophy

Since decreases in hippocampal volumes and dendritic architecture are observed in metabolic disorders (Biessels and Reagan, 2015), morphological analysis of hippocampal pyramidal neurons and DG granule neurons was performed using Golgi-Cox impregnation. In this study, each rat received the LV-Con construct in one hippocampal

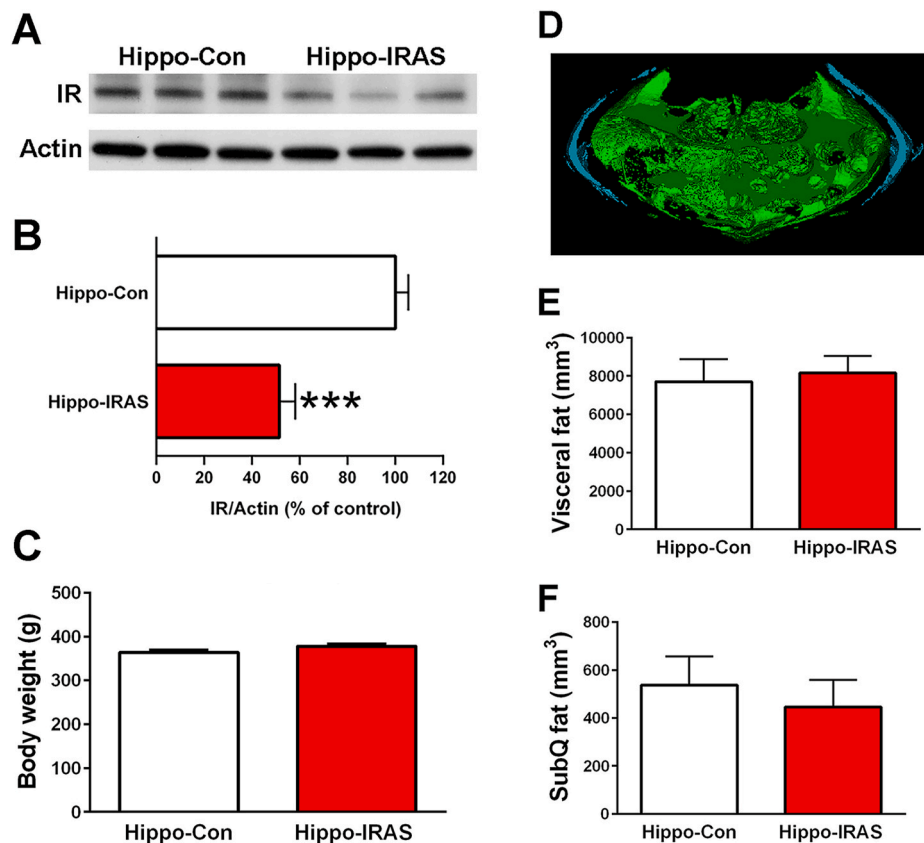


Fig. 1. Hippocampal administration of the LV-IRAS construct significantly decreases hippocampal insulin receptor expression in the absence of changes in body weight or body composition. A: Representative immunoblot for insulin receptor expression in hippocampal membrane extracts from rats that received bilateral injections of the LV-Con construct (Hippo-Con) or the LV-IRAS construct (Hippo-IRAS). Normalization for protein loading was performed using a monoclonal antibody selective for actin. B: Autoradiographic analysis determined that hippocampal insulin receptor expression is significantly decreased in Hippo-IRAS rats compared to Hippo-Con rats. (***: $p < 0.001$). C: Body weight following hippocampal virus administration did not differ between Hippo-Con and Hippo-IRAS rats ($p = 0.28$). D: Representative microCT image of visceral (green) and subcutaneous (blue) fat pads in a Hippo-Con rat. E: Volumetric analysis determined that visceral fat was not significantly different in Hippo-Con and Hippo-IRAS rats ($p = 0.76$). F: Subcutaneous fat is unchanged in Hippo-IRAS rats compared to Hippo-Con rats ($p = 0.56$). Data presented as mean \pm SEM based of at least 6 rats/group. (For interpretation of the references to color in this figure legend, the reader is referred to the web version of this article.)

hemisphere and the LV-IRAS construct in the contralateral hemisphere. Using this design, each rat served as its own control. Fig. 4 provides representative examples of a three-dimensional reconstruction of a CA3 pyramidal neuron from the LV-Con hemisphere (Fig. 4A) and the LV-IRAS hemisphere (Fig. 4B) from the same rat. Following reconstruction of Golgi-impregnated CA3 pyramidal neurons, the following parameters were evaluated: total dendritic length, total branch points, dendritic volume and dendritic complexity index (DCI), as described previously (Grillo et al., 2015b). Non-biased stereological analysis identified atrophy of the basal dendrites of CA3 pyramidal neurons in hemispheres that received the LV-IRAS construct compared to hemispheres that received the LV-Con construct. Specifically, LV-IRAS hemispheres exhibited significant decreases in total basal dendritic length (Fig. 4C), total basal branch points (Fig. 4D), basal dendritic volume (Fig. 4E), and basal dendritic complexity index (DCI; Fig. 4F) compared to hippocampal hemispheres that received the LV-Con construct. Interestingly, these structural changes were restricted to the basal dendrites of hemispheres that received the LV-IRAS construct. Apical dendrites from LV-IRAS hemispheres did not exhibit changes in total dendritic length (Fig. 4G), total branch points (Fig. 4H), dendritic volume (Fig. 4I), or dendritic complexity index (DCI; Fig. 4J) compared to hippocampal hemispheres that received the LV-Con construct.

Structural changes were also observed in the DG; representative images of impregnated granule neurons from the LV-Con hemisphere (Fig. 5A and D) and the LV-IRAS hemisphere (Fig. 5 B and E) from the same rat are shown in Fig. 5. DCI was significantly decreased in granule neurons of DGs (Fig. 5C) and DGs (Fig. 5F) in hemispheres that received the LV-IRAS construct. Additionally, DG granule neurons exhibited significant decreases in total dendritic length, total branch points and dendritic volume (Table 1). Dendritic branch points were also significantly decreased in the DGs. Collectively, these results demonstrate that downregulation of hippocampal insulin receptors restricted to a single hemisphere elicits dendritic atrophy of CA3 pyramidal neurons and DG

granule neurons.

4. Discussion

While epidemiological data support the concept that patients with metabolic disorders, such as T2DM, have an increased risk of developing neuropsychiatric disorders, the complex milieu of peripheral and central effects from these disorders makes disentangling biological components driving this comorbidity a major challenge in the field (Anderson et al., 2001; Ali et al., 2006). As insulin resistance has been proposed to be a mechanistic mediator of co-morbid depression and T2DM (Rasgon and Jarvik, 2004), the current study aimed to dissect this comorbidity link by testing whether hippocampal-specific insulin resistance directly causes hippocampal structural changes and elicits a depressive-like phenotype.

4.1. Hippocampal-specific insulin resistance decreases neurogenesis and dendritic complexity of pyramidal neurons and granule neurons

Clinical studies have highlighted that CNS structural changes are a hallmark feature in patients with metabolic disorders. For example, Biessels and coworkers reported that hippocampal formation volumes are decreased in adult T2DM patients compared to age-matched controls (Brundel et al., 2010). Similar decreases in hippocampal formation volume have been reported in adolescents with insulin resistance (Ursache et al., 2012). Rasgon and coworkers reported that insulin resistance had a significant main effect on total hippocampal volumes, and these structural changes were associated with impaired cognitive performance (Rasgon et al., 2011). A more recent study reported that the duration of T2DM, as well as the degree of glycemic control, as assessed by HbA1c levels, is correlated with decreases in hippocampal formation volume (Schneider et al., 2017). While this study did not identify structural changes in the hippocampus of participants defined as pre-diabetic,

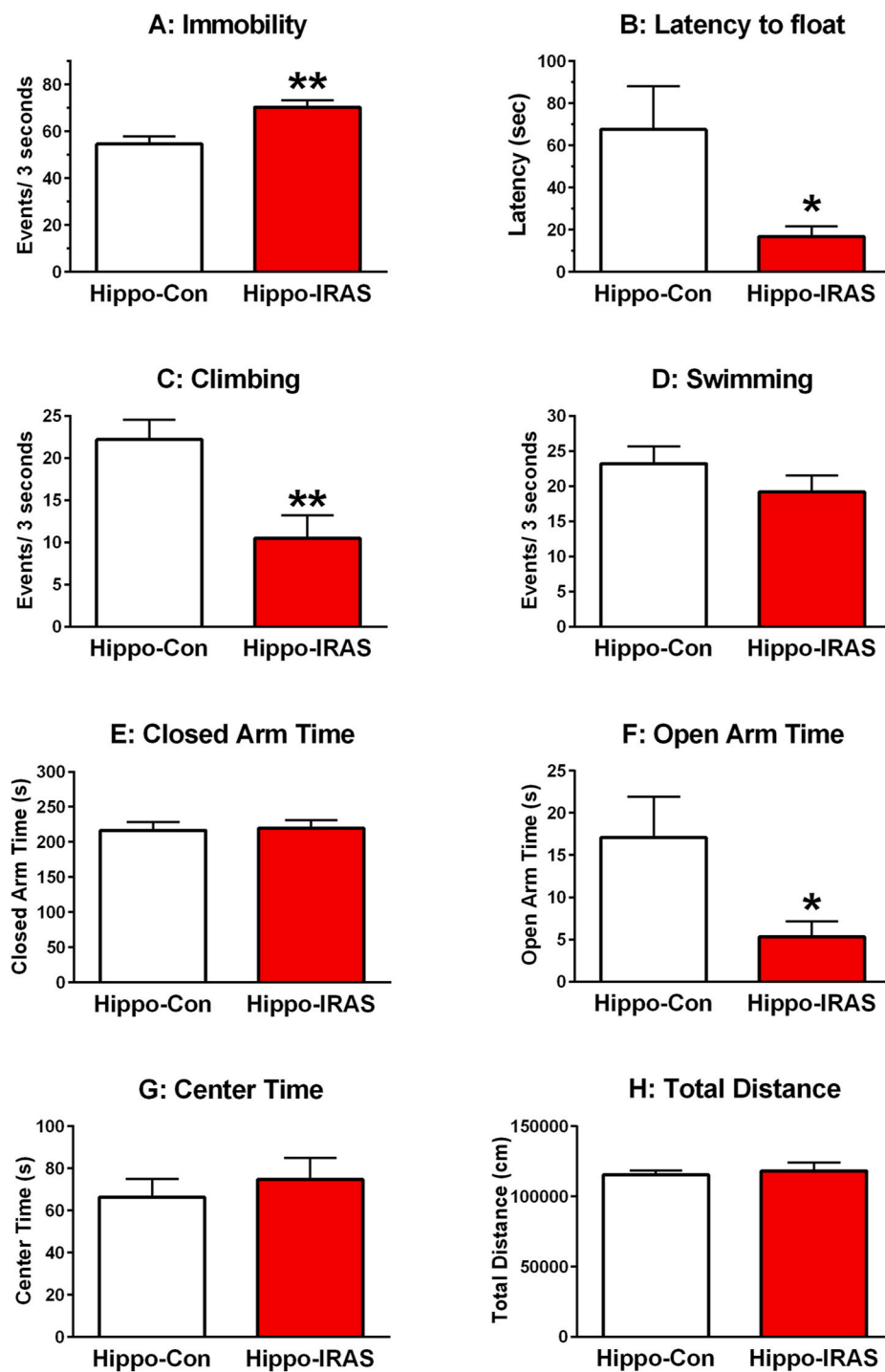


Fig. 2. Hippocampal-specific insulin resistance elicits behavioral despair and anxiety-like behaviors. A-D: Assessment of behaviors on the test day of the forced swim test (FST). A: Immobility was significantly increased in Hippo-IRAS rats compared to Hippo-Con rats (**: $p < 0.01$). B: Latency to float was significantly decreased in Hippo-IRAS rats compared to Hippo-Con rats (*: $p < 0.05$). C: Climbing was significantly reduced in Hippo-IRAS rats compared to Hippo-Con rats (**: $p < 0.01$). D: Swimming was similar in Hippo-Con and Hippo-IRAS rats ($p = 0.25$). E: In the elevated plus maze (EPM), closed arm time did not differ between Hippo-Con and Hippo-IRAS rats ($p = 0.84$). F: Hippo-IRAS rats exhibit anxiety-like behaviors as measured by decreases in open arm time, compared to Hippo-Con rats (*: $p < 0.05$). G: Time spent in the center part of the EPM did not differ between Hippo-Con and Hippo-IRAS rats ($p = 0.53$). H: Total distance traveled in the EPM did not differ between Hippo-Con rats and Hippo-IRAS rats ($p = 0.73$). Data presented as mean \pm SEM based on at least 10 rats/group.

other studies have reported decreases in hippocampal formation volume in pre-diabetic patients and T2DM patients (Dong et al., 2019). In spite of these differences, a common feature in many of these studies was that HbA1c levels were correlated with decreases in hippocampal volume.

Preclinical studies further support these clinical observations. For example, expression of depressive-like and anxiety-like behaviors have been reported in experimental models of obesity and T2DM, including *db/db* mice (Sharma et al., 2010), *ob/ob* mice (Collin et al., 2000; Yamada et al., 2011) and rodents provided access to a high fat diet (Yamada et al., 2011). Beyond the development of depressive-like and anxiety-like behaviors, rodents with metabolic disorders that include insulin resistance also exhibit morphological changes in the

hippocampus. For example, previous studies have reported that mice (Park et al., 2010; Hwang et al., 2008; Boitard et al., 2015) and rats (Lindqvist et al., 2006) provided access to a high fat diet exhibit decreases in cell proliferation and neurogenesis in the DG. Similar decreases in neurogenesis/cell proliferation were reported in *db/db* mice (Stranahan et al., 2008). Interestingly, these same investigators reported that *db/db* mice exhibit significant decreases in spine density in the DG in the absence of changes in granule cell length or branch points (Stranahan et al., 2009). Our previous studies have also identified alterations in synaptic contacts in the hippocampus of obese rodents, morphological changes that were not accompanied by neuronal degeneration (Grillo et al., 2011b). Collectively, these preclinical studies support clinical

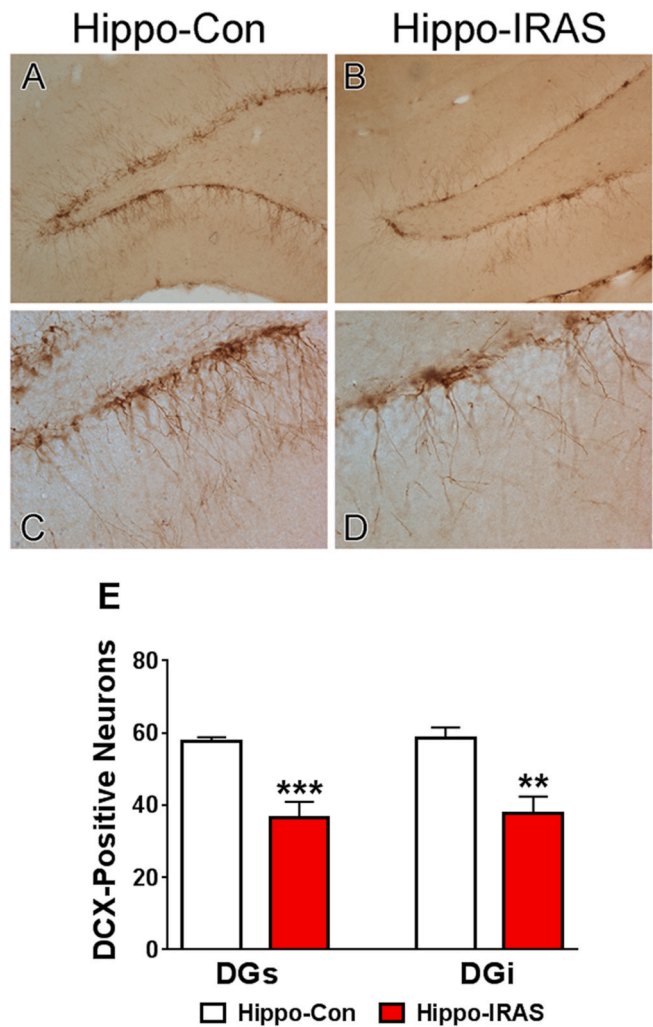


Fig. 3. The density of immature granule neurons is significantly reduced in the dentate gyrus (DG) of Hippo-IRAS rats compared to Hippo-Con rats. Representative images of doublecortin (DCX) immunohistochemistry in the DG of Hippo-Con rats (A and C) and Hippo-IRAS rats (B and D). Hippo-IRAS rats exhibit decreases in the number of DCX-positive neurons in the DG and DCX-positive neurons exhibit less complex dendritic architecture compared to Hippo-Con rats. E: Non-biased stereological counting determined that Hippo-IRAS rats exhibit significant decreases in DCX-positive cells in the superior blade of the DG (DGs, ***: $p < 0.001$) and the inferior blade of the DG (DGi; **: $p < 0.01$). Data presented as mean \pm SEM based on at least 6 rats/group.

observations which illustrate that metabolic disorders elicit structural changes in the hippocampus that are associated with the development of depressive-like behaviors.

Results from the current study both support and elaborate on these clinical and preclinical findings. By using a viral vector to specifically down-regulate insulin receptor expression in the hippocampus, we were able to disentangle central effects of insulin resistance from the plethora of peripheral complications of metabolic disorders. Our results emphasize that hippocampal-insulin resistance specifically contributes to hippocampal structural changes evidenced in these disorders. We found that hippocampal-specific insulin resistance causes reductions in the number of immature neurons suggesting hippocampal neurogenesis is decreased, and also reductions in basal but not apical dendritic

arborization of CA3 hippocampal pyramidal neurons. This decrease of neurogenesis and dendritic complexity as a result of hippocampal-specific insulin resistance may be underlying some of the global structural changes evidenced in clinical populations with metabolic disorders. Collectively, such results support the hypothesis that insulin resistance is a common feature associated with structural and functional deficits in patients with metabolic disorders (McIntyre et al., 2010).

Of note, the morphological results from Golgi impregnation represent an interesting contrast from the morphological changes elicited by chronic psychosocial stress paradigms. Previous seminal observations by McEwen and coworkers determined that chronic restraint stress induced atrophy of the apical dendrites of CA3 pyramidal neurons, but not the basal dendrites in male rats (Woolley et al., 1990). Additional studies from these same investigators demonstrated that chronic exposure to stress levels of glucocorticoids elicited similar morphological changes in the CA3 region without affecting the structural integrity of DG granule neurons (Watanabe et al., 1992). As such, these findings are in stark contrast with the current findings that identified dendritic atrophy of DG granule neurons and basal dendrites in the CA3 region. It is interesting to note that rats with hippocampal-specific insulin resistance do not exhibit changes in stress reactivity (Grillo et al., 2015a), thereby providing an important distinction between neuroendocrine causes of dendritic atrophy in psychosocial stress compared to metabolic stressors. More simply, these results demonstrate that insulin resistance, independent of alterations in HPA axis activity, may be a causative factor driving deficits in hippocampal morphological plasticity in both rodent models of and patients with metabolic disorders. This suggests that while both chronic psychosocial stress and metabolic stress reduce hippocampal formation volumes, the mechanisms underlying the structural changes which then contribute to these volumetric reductions may be fundamentally different at the cellular/synaptic level.

4.2. Hippocampal insulin resistance impacts learning and memory-based behaviors

Results from the current study are consistent with other preclinical models which have attempted to disentangle cause from consequence in insulin-resistance and its impact on neuroplasticity and behavior. For example, several studies have used molecular approaches to more selectively target brain insulin receptor populations. Surprisingly, while neuron-specific insulin receptor knockout (NIRKO) mice exhibit impairments in peripheral glucose homeostasis (Bruning, 2000), these mice do not exhibit deficits in spatial learning and memory (Schubert et al., 2004). In contrast, restricting the disruption of insulin receptor expression and signaling to the hippocampus results in significant reductions in hippocampal synaptic plasticity. In this regard, insulin receptor β -subunit haploinsufficient mice exhibit behavioral impairments in the novel object recognition test and deficits in synaptic transmission (Nisticò et al., 2012). Similarly, we have previously demonstrated that lentivirus-mediated induction of hippocampal-specific insulin resistance impairs spatial learning and eliminates stimulus-evoked long term potentiation (LTP) in the hippocampus (Grillo et al., 2015a). In both of these studies, hippocampal-specific insulin resistance was associated with alterations in the expression and phosphorylation state of glutamate receptor subunits. The current study aimed to expand on these previous findings by establishing whether hippocampal-specific insulin resistance induces a depressive-like phenotype. Interestingly, we found that while hippocampal-specific insulin resistance elicits behavioral despair in the test phase of the FST, it does not induce anhedonia. The test phase of the FST can be interpreted as a learned behavior compared to the pre-test phase which measures innate behaviors (West, 1990). Such observations are consistent with our previous studies

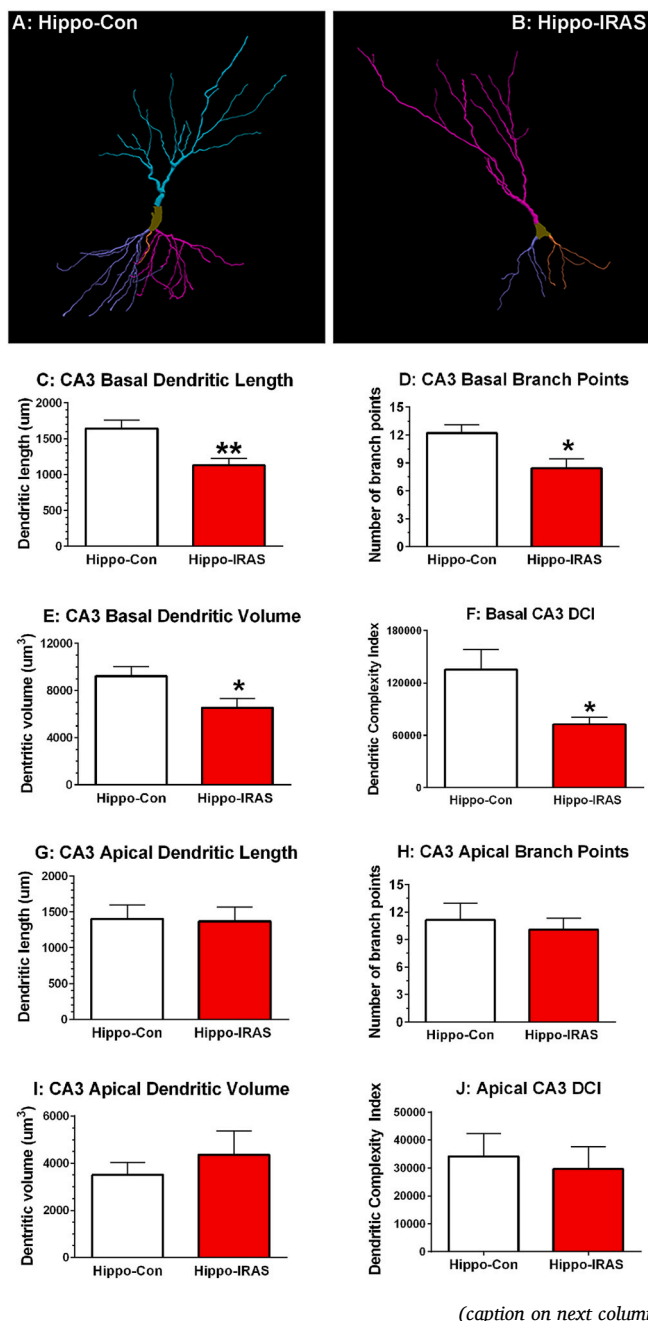


Fig. 4. Hippocampal-specific insulin resistance elicits atrophy of basal but not apical dendrites in hippocampal CA3 pyramidal neurons. Three-dimensional reconstruction of a Golgi-impregnated CA3 pyramidal neuron from the Hippo-Con hemisphere (A) and a Golgi-impregnated CA3 pyramidal neuron from the Hippo-IRAS hemisphere (B) in the same rat. Neuron summary data for the basal dendrites (C–F) of CA3 pyramidal neurons. C: Total dendritic length of basal dendrites of CA3 pyramidal neurons is decreased in Hippo-IRAS hemispheres compared to Hippo-Con hemispheres (**: $p < 0.01$). D: Basal dendritic branch points are reduced in Hippo-IRAS hemispheres compared to Hippo-Con hemispheres (*: $p < 0.05$). E: Total dendritic volume of basal dendrites of CA3 pyramidal neurons is decreased in Hippo-IRAS hemispheres (*: $p < 0.05$). F: Dendritic complexity index (DCI) of basal dendrites of CA3 pyramidal neurons of Hippo-IRAS hemispheres is significantly reduced compared to Hippo-Con hemispheres (*: $p < 0.05$). Neuron summary data for the apical dendrites (G–J) of CA3 pyramidal neurons. G: Total dendritic length of apical dendrites of CA3 pyramidal neurons are unchanged in Hippo-IRAS hemispheres compared to Hippo-Con hemispheres ($p = 0.91$). H: Apical dendritic branch points are similar in Hippo-IRAS hemispheres compared to Hippo-Con hemispheres ($p = 0.64$). I: Total dendritic volume of apical dendrites is similar in Hippo-IRAS hemispheres compared to Hippo-Con hemispheres ($p = 0.47$). J: Dendritic complexity index (DCI) of apical dendrites of CA3 pyramidal neurons of Hippo-IRAS hemispheres is not different compared to Hippo-Con hemispheres ($p = 0.70$). Data presented as mean \pm SEM based on analysis of at least 6 neurons from 5 rats.

that illustrated that insulin resistance restricted to the hippocampus elicits impairments in hippocampal dependent learning and memory (Grillo et al., 2015a) and further support the concept that hippocampal insulin receptors facilitate hippocampal synaptic plasticity, including learning and memory (McNay et al., 2010; Zhao et al., 1999). As depression is a complex disorder, impacted by a variety of neurochemical and structural alterations across multiple brain regions, the specificity of the effects of hippocampal insulin resistance on learning-based behavioral tasks provides valuable insight to the underlying molecular causes of the depressive phenotype. In addition, given the complex milieu characteristic of metabolic disorders, it is not unexpected that insulin resistance restricted to the hippocampus would not completely recapitulate the behavioral deficits observed in the experimental models of obesity described above. Indeed, it is more likely that a variety of factors are responsible for the etiology and progression of depressive-like and anxiety-like behaviors in rodents with obesity phenotypes. For example, downregulation of hypothalamic insulin receptors elicits a complex metabolic/obesity phenotype that includes decreases in brain-derived neurotrophic factor expression, increases in pro-inflammatory cytokines and leptin resistance, all of which likely contribute to the development of depressive-like and anxiety-like behaviors (Grillo et al., 2011a, 2014, 2015a). Interestingly, dietary restriction approaches that normalize obesity-induced endocrine and metabolic parameters reverse depressive-like behaviors in mice (Yamada et al., 2011) and rats (Grillo et al., 2014). Clinical studies also support this concept in that obese patients report improved mood/reduced depressive illness symptoms following bariatric surgery (Gill et al., 2019). Moreover, intranasal insulin administration has been shown to improve mood in human subjects (Benedict et al., 2004), presumably through enhancement of brain insulin signaling (Benedict and Grillo, 2018). Taken together, these clinical and preclinical studies support the notion that it is likely that many different metabolic and endocrine factors contribute to the development of depressive behaviors but also highlight a critical role of insulin resistance in neuroplasticity deficits observed in T2DM, obesity and age-related cognitive decline.

In conclusion, the results of the current study demonstrate that hippocampal-specific insulin resistance elicits structural and functional deficits in the hippocampus that are highly consistent with those observed in patients with metabolic disorders and comorbid depressive illness. As such, strategies to enhance brain insulin signaling represent a potential therapy for the restoration of neuroplasticity in patients with metabolic disorders like obesity and T2DM.

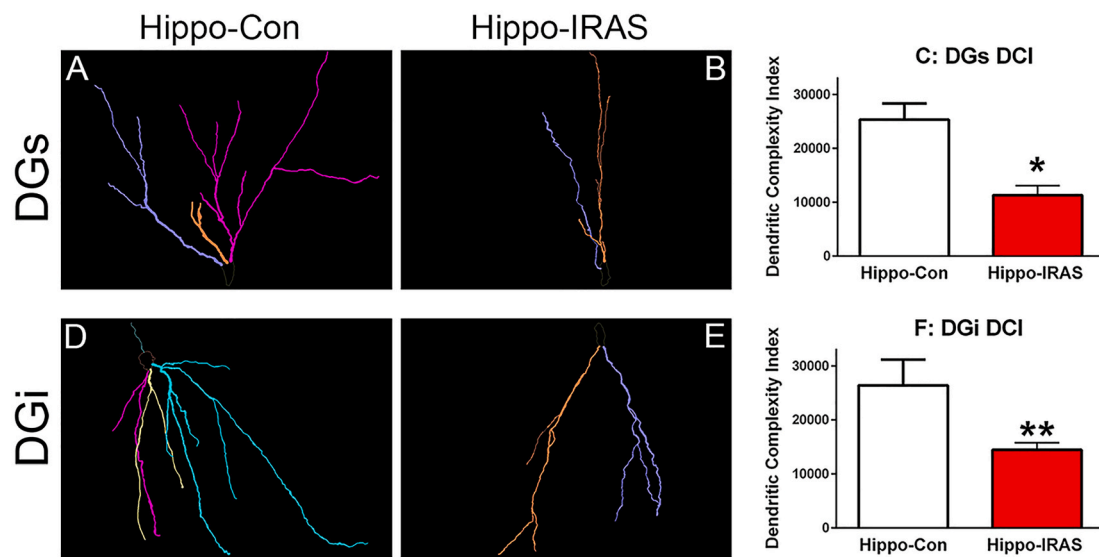


Fig. 5. Hippocampal-specific insulin resistance elicits atrophy of granule neurons of the dentate gyrus. Representative three-dimensional reconstruction of Golgi-impregnated granule neurons from the superior blade of the dentate gyrus (DGs) from a Hippo-Con hemisphere (A) and a Hippo-IRAS hemisphere (B) from the same rat. C: Dendritic complexity index (DCI) of DGs granule neurons is significantly reduced in Hippo-IRAS hemispheres compared to Hippo-Con hemispheres (*: $p < 0.05$). Representative three-dimensional reconstruction of Golgi-impregnated granule neurons from the inferior blade of the dentate gyrus (DGi) from a Hippo-Con hemisphere (D) and a Hippo-IRAS hemisphere (E) from the same rat. F: Dendritic complexity index (DCI) of DGi granule neurons is significantly reduced in Hippo-IRAS hemispheres compared to Hippo-Con hemispheres (**: $p < 0.01$). Data presented as mean \pm SEM based on analysis of at least 6 neurons from 5 rats.

Table 1

Morphometric measures of granule neurons in the superior blade of the dentate gyrus (DGs) and the inferior blade of the dentate gyrus (DGi).

		Hippo-Con	Hippo-IRAS	<i>p</i> value
DGs	Dendritic length (μm)	1320.6 \pm 143.9	1148.4 \pm 157.0	0.44
	Branch points	6.9 \pm 0.6	4.6 \pm 0.4	0.01
	Dendritic volume (μm ³)	2492.0 \pm 333.4	2434.0 \pm 107.3	0.87
	Dendritic complexity index	27258 \pm 2548	16608 \pm 2356	0.01
DGi	Dendritic length (μm)	1124.2 \pm 61.7	837.2 \pm 37.2	0.004
	Branch points	6.3 \pm 0.5	4.4 \pm 0.2	0.008
	Dendritic volume (μm ³)	2285.6 \pm 231.6	1615.8 \pm 164.7	0.04
	Dendritic complexity index	24106 \pm 2946	11924 \pm 3228	0.006

CRediT authorship contribution statement

LPR: Conceptualization, Formal analysis, Writing, Review & Editing, Supervision, Funding Acquisition. **HBC, JLW, JME, ANE, HEB, NDM, and FZLR:** Investigation. **GGP and VAM:** contributed to the discussion. **CAG:** Conceptualization, Formal analysis, Writing- Review & Editing, Supervision, Funding Acquisition. **CAG** is the guarantor of this work and, as such, had full access to all the data in the study and takes responsibility for the integrity of the data and the accuracy of the data analysis.

Funding and disclosure

Financial support for these studies was provided by the Department of Veterans Affairs grant numbers I21 BX002085, IO1 BX001804, and 1IS 1BX003556 (LPR), the National Institute of Health grant number AG066501 (JME), the National Science Foundation grant number IOS-1656626 (CAG), and the University of South Carolina Magellan Scholar Award (HBC). Any opinions, findings, and conclusions or recommendations expressed in this material are those of the authors and do not necessarily reflect the views of the U.S. Department of Veterans Affairs, the United States Government or the other stated funding agencies. The authors declare no competing financial interests.

CRediT authorship contribution statement

L.P. Reagan: Conceptualization, Formal analysis, Writing – review & editing, Supervision, Funding acquisition. **H.B. Cowan:** Investigation. **J.L. Woodruff:** Investigation. **G.G. Piroli:** contributed to the discussion. **J.M. Erichsen:** Investigation. **A.N. Evans:** Investigation. **H.E. Burzynski:** Investigation. **N.D. Maxwell:** Investigation. **F.Z. Loyo-Rosado:** Investigation. **V.A. Macht:** contributed to the discussion. **C.A. Grillo:** Conceptualization, Formal analysis, Writing – review & editing, Supervision, Funding acquisition, is the guarantor of this work and, as such, had full access to all the data in the study and takes responsibility for the integrity of the data and the accuracy of the data analysis.

Declaration of competing interest

The authors declare no competing financial interests.

Acknowledgments

Supported by the Department of Veterans Affairs grant numbers I21 BX002085, IO1 BX001804, and 1IS 1BX003556 (LPR), the National Institute of Health grant number AG066501 (JME), and the National Science Foundation grant number IOS-1656626 (CAG).

Appendix A. Supplementary data

Supplementary data to this article can be found online at <https://doi.org/10.1016/j.ynstr.2021.100354>.

References

Ali, S., Stone, M.A., Peters, J.L., Davies, M.J., Khunti, K., 2006. The prevalence of comorbid depression in adults with Type 2 diabetes: a systematic review and meta-analysis. *Diabet. Med.* 23, 1165–1173.

Anderson, R.J., Freedland, K.E., Clouse, R.E., Lustman, P.J., 2001. The prevalence of comorbid depression in adults with diabetes: a meta-analysis. *Diabetes Care* 24, 1069–1078.

Benedict, C., Grillo, C.A., 2018. Insulin resistance as a therapeutic target in the treatment of Alzheimer's disease: a state-of-the-art review. *Front. Neurosci.* 12, 215.

Benedict, C., Hallschmid, M., Hatke, A., Schultes, B., Fehm, H.L., Born, J., Kern, W., 2004. Intranasal insulin improves memory in humans. *Psychoneuroendocrinology* 29, 1326–1334.

Biessels, G.J., Reagan, L.P., 2015. Hippocampal insulin resistance and cognitive dysfunction. *Nat. Rev. Neurosci.* 16, 660–671.

Boitard, C., Maroun, M., Tantot, F., Cavaroc, A., Sauvant, J., Marchand, A., et al., 2015. Juvenile obesity enhances emotional memory and amygdala plasticity through glucocorticoids. *J. Neurosci.* 35, 4092–4103.

Bomfim, T.R., Forny-Germano, L., Sathler, L.B., Brito-Moreira, J., Houzel, J.-C., Decker, H., et al., 2012. An anti-diabetes agent protects the mouse brain from defective insulin signaling caused by Alzheimer's disease-associated A β oligomers. *J. Clin. Invest.* 122, 1339–1353.

Brundel, M., van den Heuvel, M., de Bresser, J., Kappelle, L.J., Biessels, G.J., 2010. Cerebral cortical thickness in patients with type 2 diabetes. *J. Neurol. Sci.* 299, 126–130.

Bruning, J.C., 2000. Role of brain insulin receptor in control of body weight and reproduction. *Science* 289 (80), 2122–2125.

Chen, S., Leonard, J.P., 2002. Protein tyrosine kinase-mediated potentiation of currents from cloned NMDA receptors. *J. Neurochem.* 67, 194–200.

Chiu, S.-L., Cline, H.T., 2010. Insulin receptor signaling in the development of neuronal structure and function. *Neural Dev.* 5, 7.

Collin, M., Håkansson-Ovesjö, M.L., Misane, I., Ögren, S.O., Meister, B., 2000. Decreased 5-HT transporter mRNA in neurons of the dorsal raphe nucleus and behavioral depression in the obese leptin-deficient ob/ob mouse. *Mol. Brain Res.* 81, 51–61.

Dong, S., Dongwei, L., Zhang, J., Liang, J., Sun, Z., Fang, J., 2019. Individuals in the prediabetes stage exhibit reduced hippocampal tail volume and executive dysfunction. *Brain Behav.* 9, e01351.

Ferrario, C.R., Reagan, L.P., 2018. Insulin-mediated synaptic plasticity in the CNS: anatomical, functional and temporal contexts. *Neuropharmacology* 136, 182–191.

Gill, H., Kang, S., Lee, Y., Rosenblat, J.D., Brietzke, E., Zuckerman, H., McIntyre, R.S., 2019. The long-term effect of bariatric surgery on depression and anxiety. *J. Affect. Disord.* 246, 886–894.

Grillo, C.A., Tamashiro, K.L., Piroli, G.G., Melhorn, S., Gass, J.T., Newsom, R.J., et al., 2007. Lentivirus-mediated downregulation of hypothalamic insulin receptor expression. *Physiol. Behav.* 92, 691–701.

Grillo, C.A., Piroli, G.G., Kaigler, K.F., Wilson, S.P., Wilson, M.A., Reagan, L.P., 2011a. Downregulation of hypothalamic insulin receptor expression elicits depressive-like behaviors in rats. *Behav. Brain Res.* 222, 230–235.

Grillo, C.A., Piroli, G.G., Junor, L., Wilson, S.P., Mott, D.D., Wilson, M.A., Reagan, L.P., 2011b. Obesity/hyperleptinemic phenotype impairs structural and functional plasticity in the rat hippocampus. *Physiol. Behav.* 105, 138–144.

Grillo, C.A., Mulder, P., Macht, V.A., Kaigler, K.F., Wilson, S.P., Wilson, M.A., Reagan, L.P., 2014. Dietary restriction reverses obesity-induced anhedonia. *Physiol. Behav.* 128, 126–132.

Grillo, C.A., Piroli, G.G., Lawrence, R.C., Wrighten, S.A., Green, A.J., Wilson, S.P., et al., 2015a. Hippocampal insulin resistance impairs spatial learning and synaptic plasticity. *Diabetes* 64, 3927–3936.

Grillo, C.A., Risher, M., Macht, V.A., Bumgardner, A.L., Hang, A., Gabriel, C., et al., 2015b. Repeated restraint stress-induced atrophy of glutamatergic pyramidal neurons and decreases in glutamatergic efflux in the rat amygdala are prevented by the antidepressant agomelatine. *Neuroscience* 284, 430–443.

Grillo, C.A., Woodruff, J.L., Macht, V.A., Reagan, L.P., 2019. Insulin resistance and hippocampal dysfunction: disentangling peripheral and brain causes from consequences. *Exp. Neurol.* 318, 71–77.

Hwang, I.K., Kim, I.Y., Kim, D.W., Yoo, K.-Y., Kim, Y.N., Yi, S.S., et al., 2008. Strain-specific differences in cell proliferation and differentiation in the dentate gyrus of C57BL/6N and C3H/HeN mice fed a high fat diet. *Brain Res.* 1241, 1–6.

Lindqvist, A., Mohapel, P., Bouter, B., Frielingsdorf, H., Pizzo, D., Brundin, P., Erlanson-Albertsson, C., 2006. High-fat diet impairs hippocampal neurogenesis in male rats. *Eur. J. Neurosci.* 13, 1385–1388.

Lustman, P.J., Clouse, R.E., 2005. Depression in diabetic patients. *J. Diabet. Complicat.* 19, 113–122.

Macht, V.A., Vazquez, M., Petyak, C.E., Grillo, C.A., Kaigler, K., Enos, R.T., et al., 2017. Leptin resistance elicits depressive-like behaviors in rats. *Brain Behav. Immun.* 60, 151–160.

McIntyre, R.S., Kenna, H.A., Nguyen, H.T., Law, C.W.Y., Sultan, F., Woldeyohannes, H. O., et al., 2010. Brain volume abnormalities and neurocognitive deficits in diabetes mellitus: points of pathophysiological commonality with mood disorders? *Adv. Ther.* 27, 63–80.

McNay, E.C., Ong, C.T., McCrimmon, R.J., Cresswell, J., Bogan, J.S., Sherwin, R.S., 2010. Hippocampal memory processes are modulated by insulin and high-fat-induced insulin resistance. *Neurobiol. Learn. Mem.* 93, 546–553.

Moosavi, M., Naghd, N., Maghsoudi, N., Zahedi Asl, S., 2006. The effect of intrahippocampal insulin microinjection on spatial learning and memory. *Horm. Behav.* 50, 748–752.

Nisticò, R., Cavallucci, V., Piccinin, S., Macrì, S., Pignatelli, M., Mehday, B., et al., 2012. Insulin receptor β -subunit haploinsufficiency impairs hippocampal late-phase LTP and recognition memory. *NeuroMolecular Med.* 14, 262–269.

Park, C.R., Seeley, R.J., Craft, S., Woods, S.C., 2000. Intracerebroventricular insulin enhances memory in a passive-avoidance task. *Physiol. Behav.* 68, 509–514.

Park, H.R., Park, M., Choi, J., Park, K.-Y., Chung, H.Y., Lee, J., 2010. A high-fat diet impairs neurogenesis: involvement of lipid peroxidation and brain-derived neurotrophic factor. *Neurosci. Lett.* 482, 235–239.

Pillai, A.G., Anilkumar, S., Chattarji, S., 2012. The same antidepressant elicits contrasting patterns of synaptic changes in the amygdala vs Hippocampus. *Neuropharmacology* 57, 2702–2711.

Rasgon, N., Jarvik, L., 2004. Insulin resistance, affective disorders, and Alzheimer's disease: review and hypothesis. *J. Gerontol. Ser. A Biol. Sci. Med. Sci.* 59, M178–M183.

Rasgon, N.L., Kenna, H.A., Wroolie, T.E., Kelley, R., Silverman, D., Brooks, J., et al., 2011. Insulin resistance and hippocampal volume in women at risk for Alzheimer's disease. *Neurobiol. Aging* 32, 1942–1948.

Schneider, A.L.C., Selvin, E., Sharrett, A.R., Griswold, M., Coresh, J., Jack, C.R., et al., 2017. Diabetes, prediabetes, and brain volumes and subclinical cerebrovascular disease on MRI: the atherosclerosis risk in communities neurocognitive study (ARIC-NCS). *Diabetes Care* 40, 1514–1521.

Schubert, M., Gautam, D., Surjo, D., Ueki, K., Baudler, S., Schubert, D., et al., 2004. Role for neuronal insulin resistance in neurodegenerative diseases. *Proc. Natl. Acad. Sci. U. S. A.* 101, 3100–3105.

Sharma, A.N., Elased, K.M., Garrett, T.L., Lucot, J.B., 2010. Neurobehavioral deficits in db/db diabetic mice. *Physiol. Behav.* 101, 381–388.

Skeberdis, V.A., Lan, J.-y., Zheng, X., Zukin, R.S., Bennett, M.V.L., 2001. Insulin promotes rapid delivery of N-methyl-D-aspartate receptors to the cell surface by exocytosis. *Proc. Natl. Acad. Sci. Unit. States Am.* 98, 3561–3566.

Stranahan, A.M., Arumugam, T.V., Cutler, R.G., Lee, K., Egan, J.M., Mattson, M.P., 2008. Diabetes impairs hippocampal function through glucocorticoid-mediated effects on new and mature neurons. *Nat. Neurosci.* 11, 309–317.

Stranahan, A.M., Lee, K., Martin, B., Maudsley, S., Golden, E., Cutler, R.G., Mattson, M.P., 2009. Voluntary exercise and caloric restriction enhance hippocampal dendritic spine density and BDNF levels in diabetic mice. *Hippocampus* 19, 951–961.

Talbot, K., Wang, H.-Y., Kazi, H., Han, L.-Y., Bakshi, K.P., Stucky, A., et al., 2012. Demonstrated brain insulin resistance in Alzheimer's disease patients is associated with IGF-1 resistance, IRS-1 dysregulation, and cognitive decline. *J. Clin. Invest.* 122, 1316–1338.

Tanis, R.M., Piroli, G.G., Day, S.D., Frizzell, N., 2015. The effect of glucose concentration and sodium phenylbutyrate treatment on mitochondrial bioenergetics and ER stress in 3T3-L1 adipocytes. *Biochim. Biophys. Acta Mol. Cell Res.* 1853, 213–221.

Ursache, A., Wedin, W., Tirsii, A., Convit, A., 2012. Preliminary evidence for obesity and elevations in fasting insulin mediating associations between cortisol awakening response and hippocampal volumes and frontal atrophy. *Psychoneuroendocrinology* 37, 1270–1276.

Watanabe, Y., Gould, E., McEwen, B.S., 1992. Stress induces atrophy of apical dendrites of hippocampal CA3 pyramidal neurons. *Brain Res.* 588, 341–345.

West, A.P., 1990. Neurobehavioral studies of forced swimming: the role of learning and memory in the forced swim test. *Prog. Neuropsychopharmacol. Biol. Psychiatr.* 14, 863–877. IN3-IN4.

Woolley, C.S., Gould, E., McEwen, B.S., 1990. Exposure to excess glucocorticoids alters dendritic morphology of adult hippocampal pyramidal neurons. *Brain Res.* 531, 225–231.

Yamada, N., Katsuura, G., Ochi, Y., Ebihara, K., Kusakabe, T., Hosoda, K., Nakao, K., 2011. Impaired CNS leptin action is implicated in depression associated with obesity. *Endocrinology* 152, 2634–2643.

Zhao, W., Chen, H., Xu, H., Moore, E., Meiri, N., Quon, M.J., Alkon, D.L., 1999. Brain insulin receptors and spatial memory. *J. Biol. Chem.* 274, 34893–34902.